POLITECNICO DI TORINO
Repository ISTITUZIONALE

Escaping alpha-particle monitor for burning plasmas

Original
Escaping alpha-particle monitor for burning plasmas / Kiptily, V.G., Shevelev, A.E., Goloborodko, V., Kocan, M., Veshchev, E., Craciunescu, T., Khilkevitch, E.M., Lengar, I., Polunovsky, I.A., Schoepf, K., Soare, S., Yavorskij, V., Zoita, V.L., Subba, F.. - In: NUCLEAR FUSION. - ISSN 0029-5515. - 58:8(2018). [10.1088/1741-4326/aab676]

Availability:
This version is available at: 11583/2986815 since: 2024-03-11T16:28:48Z

Publisher:
IOP PUBLISHING LTD

Published
DOI:10.1088/1741-4326/aab676

Terms of use:

This article is made available under terms and conditions as specified in the corresponding bibliographic description in the repository

Publisher copyright
IOP preprint/submitted version

This is the version of the article before peer review or editing, as submitted by an author to NUCLEAR FUSION. IOP Publishing Ltd is not responsible for any errors or omissions in this version of the manuscript or any version derived from it. The Version of Record is available online at https://dx.doi.org/10.1088/1741-4326/aab676.

(Article begins on next page)

16 November 2026

Escaping alpha-particle monitor for burning plasmas

V G Kiptily[1], A E Shevelev[2], V Goloborodko[3], M Kocan[4], E Veshchev[4], T Craciunescu[5], E M Khilkevitch[2], I Lengar[6], I A Polunovsky[2], K Schoepf[3], S Soare[5], V Yavorskij[3, a], V L Zoita[5] and JET contributors[b]

[1] CCFE, Culham Science Centre, Abingdon, OX14 3DB, UK
[2] Ioffe Institute, Politekhnicheskaya 26, St. Petersburg 194021, Russian Federation
[3] OEAW, Institute for Theoretical Physics, University of Innsbruck, Austria
[4] ITER Organization, 13067 St Paul Lez Durance Cedex, France
[5] Institute of Atomic Physics, Bucharest, Romania
[6] Jozef Stefan Institute, Reactor Physics Department, Ljubljana, Slovenia

[a] Now deceased.
[b] See the author list of [36]

E-mail: vasili.kiptily@ukaea.uk

Abstract. This paper presents a diagnostic system, Gamma-Ray Alpha-particle Monitor (GRAM), for continuous monitoring of deuterium-tritium fusion α-particles in the MeV energy range escaped from the plasma to the first wall. The diagnostic is based on the detection of γ-rays produced in nuclear reactions. The reactions ^{9}Be(α,nγ)^{12}C and ^{10}B(α,pγ)^{13}C have been selected. For that purpose, Be- or ^{10}B-target is placed on the first wall, where the alphas are expected to be mostly lost. Striking the target, the lost alphas generate specific γ-rays, if their energy E_α > 1.5 MeV. To measure this γ-ray emission, the target should be in the field of view of a collimated detector, which is protected from neutrons and background gammas. The calibrated detector could deliver absolute values of the lost α-particle flux with a temporal resolution depending on intensity of losses. A high-performance γ-ray spectrometer with a novel architecture, GRITER, is proposed to be used in GRAM. It consists of a stack of the optically isolated high-Z fast scintillators with independent signal readout. GRITER is supposed to be operated at count-rates substantially exceeding the capability of a single crystal detector of the same size. The GRAM diagnostic system consists of two identical spectrometers, which measure both γ-rays due to α-particle loss and γ-ray background ensuring reliable data in a harsh reactor environment. GRAM could be tested during the non-DT plasma operation monitoring lost DD fusion products, neutral beam heating D-ions (E_D > 0.5 MeV) and ICRF accelerated H- and ^{3}He-ions through the detection of γ-rays resulting from nuclear reactions. The use of GRAM on JET and ITER, including events with extremely high loss rates, is discussed.

1. Introduction

Fusion reactors with magnetic confinement of burning plasma will have diagnostics used for machine protection and plasma control. In deuterium-tritium plasmas, 3.5-MeV α-particles are a primary source of the plasma self-heating, transferring energy to the plasma and they should be under continuous monitoring. Diagnosing behaviour of α-particles in the plasma, i.e. changes in slowing down and redistribution of confined particles, their escape to the first wall, is a big challenge especially in reactors characterised by a harsh radiation environment [1, 2]. In this paper, we are focusing on the diagnostics for continuous monitoring of escaping

α-particles, in particular in the Joint European Torus (JET) and the experimental fusion reactor ITER that is being constructed to demonstrate the feasibility of magnetically confined fusion as a source of energy.

The importance of the fusion α-particle loss measurements arises from the necessity of the plasma control and wall protection. Indeed, increases in the loss-to-neutron ratio indicate changes of the magnetic field configuration or/and plasma parameters that lead to degradation of the plasma performance. Also, slow magnetohydrodynamics (MHD) fluctuations can cause a loss rate rise that requires a response of plasma control system. However, the loss rate can change very rapidly due to resonant interactions between MHD perturbations and α-particles, e.g. high-frequency waves Toroidal Alfvén Eigenmodes, or non-resonant interactions, when MHD perturbations are driven by thermal plasma or fast particles other than the α-particles. Both mechanisms could lead to a blast of particle ejection, which is strongly localised, and therefore can cause erosion of the first wall and reduce the fusion reactor performance.

In ITER the first wall power loads resulting from escaping alphas and other fast ions, e.g. neutral beam ions, will be monitored by means of infra-red (IR) cameras viewing the first wall. This diagnostic will measure the integral load, which will depend partly on the alpha-particle loss rate, but will not be able to separate the escaping α-particle loss from other type of wall loads. That is why the IR measurements are not suitable for the fusion power control or for physics studies because detailed information on escaped alphas is needed for understanding of processes causing the losses.

There are two types of lost energetic ion detectors which are used on large tokamaks (JET, ASDEX-Upgrade etc.): thin foil collectors, Faraday Cups [3] and Scintillator Probe, or fast ion loss detector, FILD [4-6]. The Faraday Cups detects integral current of lost fast ions with energy resolution restricted by number and thickness of the foils. FILD can provide the energy and pitch-angle resolution of lost fast ions and α-particles. In ITER, a detector fixed on the wall would be exposed to continuous high plasma heat load, which is intolerable for a FILD and the only solution is to mount the detector head on a reciprocating drive system allowing the loss measurements for a short period defined by the heat resistance of the probe. A feasibility study for FILD in ITER has been carried out [7].

In this paper we present a novel diagnostic technique for continuous monitoring of α-particle losses, Gamma-Ray Alpha-particle Monitor (GRAM), which could be additional to FILD, providing important information on permanent basis, especially at extremely high heat loads to the wall, when FILD cannot be used.

Section 2 presents some results of modelling and assessments of escaping α-particles in ITER and JET discharges. In section 3 we describe the GRAM diagnostic method and its range of applicability. In section 4 we present a novel architecture of the γ-ray detector for ITER (GRITER) and outline possible neutron shielding materials. Generic GRAM locations for use in ITER and JET and the diagnostic performance assessments are discussed in section 5. Finally, we discuss the potential and drawbacks of GRAM in section 6.

2. Escaping fusion alpha-particles

The evaluation of the escaping fusion α-particle impact on the first wall predicts the low level of the first orbit (FO) and cone losses in ITER, however the neoclassical diffusive/convective loss also will be significant. The α-particle diffusive loss is substantially enhanced by toroidal field (TF) ripples [8, 9]. In JET the situation is different, the FO losses of fusion products are dominant. Indeed, in JET the TF ripples are rather small $\delta \equiv (B_{max} - B_{min})/(B_{max} + B_{min}) < 0.1\%$, whereas in ITER it is expected to be $\delta \sim 0.75\%$ without special ferritic inserts to be used for the mitigation of the TF distortion. Also, it is well known that MHD perturbations can cause continuous and massive bursting losses [10, 11], which are toroidally symmetric but poloidally could be strongly localised. Thus, the radial transport of fast particles is crucial for the charged fusion products heat deposition on the first wall, since it results in a strong localization of the escaping ions.

Modelling based on the 3D steady state Fokker–Planck code in the constants-of-motion space approach [12, 13] shows that in ITER the fraction of fusion alphas lost on the first orbit together with cone losses is less than 1% [14]. Nevertheless, the radial diffusive and convective losses are predicted to take place at a narrow range of poloidal angles below midplane and are strong ~ 10-20%. Figure 1 shows the fraction of α-particles lost with energies higher than E, and their energy spectra for the standard H-mode (2^{nd} scenario) and steady-state (4^{th} scenario) plasmas in ITER [15] calculated in the approximation with a mono-energetic birth spectrum. One can see that alphas in energy ranges 0.5 – 1 MeV and 3 – 3.5 MeV contribute predominantly to collisional losses. In the wide energy range the total neo-classical diffusion loss for the 4^{th} scenario is about 31 % vs 24 % loss fraction for the 2^{nd} scenario.

The α-particle birth spectrum is rather broad because of the DT reaction kinematics at the high plasma temperature and beam-target/beam-beam contributions. The thermal DT reaction in ITER is dominant and in the plasma core the full width at half-maximum of the α-particle source energy spectrum is ~ 1.7 MeV. Energy spectra of lost alphas (Fig.2) and the loss fraction (Fig.3) were calculated with a realistic α-particle source in 2^{nd} scenario. Figure 3

shows an enhancement of fraction of collisional losses with $E_\alpha > 1$ MeV and a reduction in the range $E_\alpha < 1$ MeV. In figure 3 we present the fraction of α-particle losses calculated with different TF ripple parameter δ in 2nd scenario. One can see that substantial losses in the MeV energy range, i.e. up to 9 % of alphas with $E_\alpha > 1.5$ MeV could be lost with TF ripple δ = 0.7%, and negligible losses for the case δ = 0.2%, which could be realised with ferritic inserts.

3. Diagnostic method

The gamma-ray alpha-particle monitor, GRAM, could be used for continuous monitoring of α-particles in the MeV energy range, escaping from the burning plasma to the first wall (FW). The diagnostic is based on the detection of γ-rays produced due to nuclear reactions in a special target placed on the first wall, where the alphas are expected to be mostly lost. Gamma-rays produced by alphas propagate through the target/tile and neutron shielding with minor attenuation to the detector. The calibrated diagnostics can provide absolute values of α-particles flux to the wall with temporal resolution depending on intensity of losses in the MeV range.

Measurements of escaping α-particle velocities with nuclear reaction $^{9}Be(\alpha,n\gamma)^{12}C$ by means of the Doppler shape analysis of broadened γ-ray peak in the recorded spectrum has been proposed in [16]. Also, the use of γ-rays from the $^{10}B(\alpha,p\gamma)^{13}C$ reaction was considered to infer the α-particle loss flux in ITER [17].

The applicability of these nuclear reactions for the α-particle diagnostics is determined by their cross-sections. The beryllium target is most promising due to a high cross-section of the reaction $^{9}Be(\alpha,n\gamma)^{12}C$ (Fig.4). The escaped fusion alphas striking the Be-target create the ^{13}C nuclei in different excited states that decay by neutrons to excited ^{12}C nuclei (Fig.5). Neutrons populate the first excited state of ^{12}C nucleus, having spin and parity $J^\pi = 2^+$, which then is discharged by 4.438-MeV γ-rays, and second one, 0^+ that is feeding the 2^+ state due to the γ-ray transition with energy 3.214 keV. From figure 4, representing partial cross-sections of this nuclear reaction, one can see that the highest probability to react fusion alphas with Be in the target takes place at $E_\alpha = 1.88$ MeV. This resonance in the cross-section is rather broad, having width $\Gamma_{cm} \sim 0.22$ MeV, thus α-particles with $E_\alpha > 1.7$ MeV (the lost fraction ~ 8.5% at the TF ripple δ=0.7%) could produce 4.44-MeV gammas. The excitation probability of the state 0^+ with generation of the 3.21-MeV gammas is much lower and became valuable for particles with $E_\alpha > 4$ MeV (the lost fraction ~ 1%).

A boron target enriched with isotope ^{10}B is also attractive for use in the diagnostics because γ-rays discharge three levels populated by protons in the $^{10}B(\alpha,p\gamma)^{13}C$ reaction (Fig.6) with comparable probabilities (Fig.7). In practice, α-particles with E_α = 1.5 MeV give rise to 3.85-MeV γ-rays, while population of two other levels is poor; at E_α = 2.3 MeV probability of generation of 3.68-MeV gammas become higher than 3.85-MeV gammas; at E_α = 3 MeV all gammas are produced though 3.85-MeV is most intensive; at E_α = 4 MeV the 3.85-MeV gammas dominate. It is important to mention that α-particles with E_α > 3.5 MeV give rise to 3.50 MeV and 3.55 MeV gammas due to the $^{10}B(\alpha,n\gamma)^{13}N$ reaction for which the cross-section is presented in figure 8. Despite α-particles producing the most intensive γ-ray response in Be target, the use of ^{10}B one gives some advantages. First, the cross-section of the $^{10}B(\alpha,p\gamma)^{13}C$ reaction is rather valuable for the detection of α-particles with energies $E_\alpha \geq 1.5$ MeV; second, a variety of gammas with different excitation functions make it possible to infer the energy distribution of the lost α-particles.

It is important to note that an application/test of the GRAM system is possible during the non-DT operation. Lost DD fusion products (protons, tritons), neutral beam heating D-ions, ICRF accelerated H- and ^{3}He-ions could be measured by means of the following nuclear reactions $^{9}Be(p,\gamma)^{10}B$, $^{9}Be(p,\alpha\gamma)^{6}Li$, $^{9}Be(d,n\gamma)^{10}B$, $^{9}Be(d,p\gamma)^{10}Be$, $^{9}Be(t,\gamma)^{11}B$, $^{9}Be(^{3}He,p\gamma)^{11}B$ and $^{9}Be(^{3}He,n\gamma)^{11}C$.

4. Gamma-ray detector

For the fusion α-particle loss measurements the diagnostic target is installed in the field of view (FoV) of a collimated detector. An identical detector, which does not see the diagnostic target, i.e. “blind” detector, needs to be installed to provide γ-ray background measurements to be compared with α-particle monitor. Both detectors should be well protected from the direct neutrons, coming from the vessel through the collimators and side neutrons scattered in the reactor structure.

The feasibility of the α-particle monitoring depends on efficiency of the neutron suppression of the direct neutrons and neutron induced γ-ray background. The best neutron shielding is the enriched lithium-6 hydrate, ^{6}LiH, however LiH with a natural Li isotope composition can be used as well. It is an extremely effective neutron attenuator with a high transparency for MeV γ-rays. Practically, it does not generate γ-rays in the MeV-energy range by itself. Measurements show that 30-cm sample of the ^{6}LiH-filter reduces 2.5-MeV neutron flux ~900 times and the 15-MeV neutron flux ~30 times [21]. The ^{6}LiH attenuator installed in

JET has demonstrated excellent results in the deuterium plasma experiments [22]. Indeed, the neutron induced background reduction in the energy range below 3 MeV was a factor of 100. A small reduction of γ-ray intensity (factor of 2) occurred in the energy range above 3 MeV, which is defined by γ-ray transparency of the attenuator.

Also, pure water (PW) can be used as an attenuator of 14.1-MeV DT fusion neutrons. Such PW neutron attenuators have been developed and implemented for the JET gamma-ray cameras [23]. A drawback of the PW neutron shield is water activation due to the $^{16}O(n,p)^{16}N$ reaction, which has 10-MeV threshold. As a result, β-decay ($T_{1/2}$ = 7.13 s) of ^{16}N leads to the generation of 6.13-MeV gammas discharged excited ^{16}O nuclei. However, for GRAM an advantage of the PW attenuator is that it could be of variable length/thickness depending on the reactor fusion power. In this case there is a possibility to optimise neutron attenuation and γ-ray transparency and thus get an increase of the signal-to-background ratio.

There are specific requirements for GRAM with Be-target. It is important to note that the detector line of sight (LoS) in ITER should not intersect the plasma region with high DT fusion rate because the confined alphas with E_α > 1.7 MeV interact with Be, which is a main plasma impurity, in the same way as lost particles in the Be-target, contaminating the loss monitor data. Also, the data can be affected if there is a large amount of carbon-containing material in the monitor FoV. Indeed, neutrons with energy exceeding 4.5 MeV can produce an unwelcome background of 4.44-MeV γ-rays from the inelastic scattering reaction $^{12}C(n,n'\gamma)^{12}C$.

The main criteria in selecting the γ-ray detector for GRAM are detection efficiency, energy and time resolution and radiation resistance. Up to date the best detector for the DT operation is a fast high-Z heavy scintillator $LaBr_3(Ce)$, known as "BriLanCe", which has short light decay time of ~20 ns that allow a high rate γ-ray detection. An enormous light output of LaBr3(Ce) scintillator provides an extremely good energy resolution of the detector ~ 4% at E_γ = 0.662 MeV; it is practically insensitive to neutrons (since nuclear reaction cross-sections are much less than those of γ-ray interaction) and the radiation resistance exceeds 1 Mrad SI-equivalent dose.

Recently, high resolution spectra at count-rates up to 10 MHz have been recorded during hard X-ray measurements with $LaBr_3(Ce)$ crystal coupled to a photo-multiplier tube (PMT) [24, 25]. Also, the latest developments of compact spectrometers based on $LaBr_3(Ce)$ scintillator crystal coupled to a silicon photo-multiplier (SiPM) [26-28] show promising results,

allowing γ-ray pulse height analysis at count-rates up to 3 MHz with energy resolution of 3%-4% in the 3-5 MeV range [28].

Here, we propose a novel architecture of the γ-ray detector for ITER, GRITER (Fig.9) to provide an advanced high count-rate and peak-to-background ratio spectrometry. It consists of a stack of optically isolated high-Z fast scintillators, i.e. $LaBr_3$(Ce), of the optimized thickness and number. Each section has an independent signal readout equipped with a fast digitiser. Since every detector section can operate at multi-MHz count-rates, GRITER could substantially exceed the capabilities of a single-crystal detector of the same size. An advantage is a possibility to increase peak-to-background ratio, processing signals in the Compton scattering suppression (CSS) or in the full energy modes. This spectrometer can be operated both in real-time and post processing modes.

Using the Monte Carlo radiation transport code (MCNP) [29], an optimal thickness of the section has been defined as about 1 cm for 8-section GRAM. Some response functions for the 1-cm thick $LaBr_3$(Ce) detector having cross-section 4 x 4 cm^2 for γ-rays with E_γ = 4.44, 6.8 and 9 MeV are shown in figure 10. One can see that the most intensive peaks in MeV γ-ray spectra are single escape ($E_{SEP} = E_\gamma - m_e c^2$) and double escape ($E_{DEP} = E_\gamma - 2m_e c^2$) peaks related to the escape from the detector of one or both 511-keV positron annihilation photons. A continuous Compton scattering background under SE and DE peaks of 4.44-MeV gammas produced by more energetic photons is one of the main concerns for spectrometry in fusion devices because of intensive γ-ray background emission up to ~ 9 MeV generated by neutrons.

5. Generic GRAM location and performance

There is a unique possibility to implement and test GRAM on JET during the planned DT experiments. JET is now equipped with ITER-like wall that means most parts of the vessel are covered by beryllium tiles and these tiles can be used as a target for GRAM. One possible position of the monitor is on the top of the machine, where the collimated detector and shielding can be installed. In this case LoS of the detector could intersect the Be-limiter as shown on figure 11. Modelling of fusion α-particles in JET plasmas [30] shows that FO and cone losses dominate on JET (Fig.12). However, losses with E_α > 1.7 MeV, due to radial diffusive/convective transport, are localised in rather narrow range of poloidal angles 0°- 30° below the midplane (Fig.13). Studies of an enhancement of these losses in a special high ripple experiment [31] would be very important for ITER developments.

According to a conservative assessment, the neoclassical losses in JET are expected to be ~ 4% - 6%, compare to a FO loss flux ~ 25%. The total averaged alpha-particle loss flux on

the limiter just below midplane (with maximum at poloidal angle ~ 5^0) is about $2x10^{-3}$ m^{-2} s^{-1} per DT neutron in the 2.5 MA plasma discharge. In this case, area of the limiter viewed by GRAM is predicted to emit 4.44-MeV γ-rays of the $^9Be(\alpha,n\gamma)^{12}C$ reaction with rate ~ $6x10^{-9}$ m^{-2} s^{-1} per DT neutron. This is a continuous rate expected for a quiet plasma discharge without any perturbations, however this rate can be ten times higher during some MHD [11], triggering anomalous α-particle losses.

It is important to note that the JET divertor consist of carbon tiles covered by tungsten. Modelling shows that 1 g of carbon will produce background γ-rays due to the $^{12}C(n,n'\gamma)^{12}C$ reaction with rate ~10^{-8} s^{-1} per DT neutron. Thus, any LoS for GRAM intersecting the JET divertor or other carbon-containing structures could create a complicated background problem. Recently, the implementation on JET of such a technique for the monitoring of the lost alphas has been extensively evaluated during a comprehensive feasibility study and conceptual design [32, 33]. Available technical solutions at that date have shown how critical was the choice of LoS in tokamak with carbon parts.

As to ITER, there is no possibility to find a similar top view of Be-wall. However, GRAM could be placed in the port occupied by detectors of the radial neutron camera (RNC). A generic line of sight of GRAM is depicted in figure 14. The monitor, which consist of two detectors, one for α-particle loss measurements and a "blind" for the γ-ray background control, could be placed in the upper in-port cassette. The Be-target could be a FW-like tile covering a part of the diagnostic port (Fig.15). Both detectors would be equipped with identical collimators, filled with neutron attenuator based on LiH or pure circulating water. The length of the PW attenuators could be variable; the level of water is controlled by the expected fusion power. In the 150-cm PW attenuator, neutrons with $E_n > 0.1$ MeV are suppressed by factor ~ $5x10^{-7}$; the attenuation factor for 4.44-MeV gammas ~$7x10^{-3}$.

Modelling 4.44-MeV gammas produced by alphas in the Be-target and the γ-ray background, which is related to interaction of neutrons with materials of the reactor structures, shielding and the detector has been carried out with MCNP code. In the model the port-plug is a generic shielding composed of steel and water (80% SS + 20% H_2O). The 4-cm circular collimators are in a cassette, which is identical to the upper in-port cassette proposed for the RNC [34]. In these conservative assessments we consider that the parallel 14.1-MeV flux of DT neutrons is normal to the port-plug and tungsten divertor, which is seen by the detectors. Also, we directed the parallel neutron flux along the collimators. In the first approximation an isotropic 4.44-MeV γ-ray emission from the Be-target is assumed. Calculations of γ-ray

background spectra recorded in the front GRITER section during the 500 MW discharge with DT neutron rate $R_{DT} = 1.8x10^{20}$ is presented in figure 16. One can see that main contributions to the total background make the γ-ray emission from the FoV spot on the tungsten divertor and side gammas generated by neutrons in the port-plug. Many fewer γ-rays are produced by neutrons in the 150-cm PW collimator (direct gammas) and in detector itself (direct neutrons). It was found that total expected background count-rate ~ $5x10^5$ s^{-1}.

The signal, 4.44-MeV γ-rate, has been estimated assuming results of calculations made for the α-particle loss fraction in 2nd ITER scenario with TF ripple parameter $\delta = 0.7\%$. This simulation is based on Monte-Carlo modelling of the diffusive loss of marginally confined fast ions which accounts for pitch-angle scattering and TF ripples. In the axisymmetric limit the neoclassical losses of alphas with $E_\alpha > 1.7$ MeV are localised near the mid-plain, Z = 0.52m, as it shown in figure 17, in the narrow poloidal range $\Delta Z \sim 0.6$ m related to $\Delta\theta \sim 4^0$. The calculated averaged flux of alphas with $E_\alpha > 1.7$ MeV is expected to be $F_\alpha \approx 2.6x10^{-3}$ m^{-2} per DT neutron. Thus, in the 500 MW discharge $F_\alpha \approx 4.7x10^{17}$ $m^{-2}s^{-1}$ that is an equivalent to the heat load ≈ 180 kW m^{-2} due to the α-particles with E_α>1.7MeV.

Considering the simulated background γ-ray emission and the α-particle loss flux on Be-target, we calculated 4.44-MeV γ-ray spectra to be recorded by GRITER. The integral spectra for two options of 125-cm collimator, with PW and LiH neutron attenuators, are presented in figures 18 and 19, consequently. The calculations were made for the 500 MW discharge (scenario #2) with 1 MW m^{-2} loss of α-particles with $E_\alpha > 1.7$ MeV. These are spectra with energy resolution $\Delta E_\gamma/E_\gamma$=0.04. They are recorded in the anti-coincidence mode, i.e. the Compton scattered gammas detected in any other section of GRITER are rejected. Using this mode, a substantial suppression of both internal and external background was achieved, delivering best signal-to-background ratio. One can see that the LiH collimator provides a stronger signal than the pure water one. However, at the same time background at ~ 2 MeV is much higher. This difference is due to LiH having a better γ-ray transparency than PW in the MeV range.

Both the total count-rate and the signal-to-background ratio define the time resolution of the spectrometer, i.e. how long the spectrum should be recorded to get the required accuracy of the data, $\Delta t = (\sqrt{B} + \sqrt{S+B})^2/S^2\varepsilon^2$; where S and B are the peak and background under the peak count-rates; ε – the required accuracy. The calculated spectra presented in figures 18 and 19 show that $\Delta t_{DEP} \approx 30$ ms is needed for 10% accuracy of DEP recorded by GRITER with PW attenuator. For the case with LiH attenuator the time resolution is $\Delta t_{DEP} \approx 10$ ms. Indeed,

GRAM monitor data is a sum of the DEP, SEP and FEP contributions, thus expected time resolution is much better, $\Delta t_{PW} \approx 13$ ms and $\Delta t_{LiH} \approx 4$ ms, consequently. It is important to note that it is rather straightforward to assess the GRITER time resolution for any strength of the losses using the above data. In the first approximation $\Delta t \approx [F_\alpha\,(1MW)/F_\alpha]^2 \Delta t(1MW)$. Thus, for example, for 100 kW m^{-2} α-particle loss the spectra should be recorded during the $\Delta t_{PW} \approx$ 1.3 s in the case of the PW attenuator and $\Delta t_{LiH} \approx 0.4$ s with LiH one to deliver data with accuracy 10%.

In the case of the ^{10}B-target the expected time resolution will be a bit worse due to the lower reaction cross-section. However, the use of this target is more beneficial to infer the lost α-particle energy distribution.

6. Discussion

The presented novel technique has some benefits and drawbacks like any other fusion reactor diagnostics. This is a rather simple and robust diagnostic, which does not require an access to the vacuum vessel, can provide continuous α-particle monitoring in the broad range of loss fluxes, from quiet to transient plasmas with extremely high loss rate and heat load. Assessments show that GRAM satisfies the ITER requirements [35], i.e. measurement of lost α-particles with temporal resolution Δt=100 ms with 10% accuracy in steady plasmas and Δt=10 ms with 30% accuracy at transient conditions. The time resolution of the GRAM improves with increasing loss rate, thus during MHD instabilities with high bursting losses its data could become important for fast alpha-particle studies (e.g. fishbones, Alfven Eigenmodes etc.). It is important that the "blind" detector, measuring γ-ray background, can ensure credible data in a harsh reactor environment.

GRITER, a high performance γ-ray spectrometer based on the detector array, is beneficial for the GRAM, nonetheless it could be used in other applications at high γ-ray loads. The proposed architecture of the device makes it possible to obtain rather promising spectrometric parameters with state-of-arts components.

It is essential to emphasise that GRAM can be also used for fast ion loss studies in plasmas other than deuterium-tritium. It could be DD fusion products, ICRF accelerated ions (H, D, ^{3}He, ^{4}He) and neutral beam heating D-ions ($E_D > 0.5$ MeV). For example, mimicking α-particles, the diagnostics can be tested and calibrated to be used in future DT plasma experiment.

The main drawback of the diagnostic is a restricted energy range of lost α-particles (E_α > 1.5 or 1.7 MeV) and lack of energy resolution since slowing down of α-particles in the target leads to integration of the γ-ray yield. Second, this technique does not provide information about the pitch-angle distribution of losses. However, high energy resolution detectors could be used in DD experiments. That allows inferring pitch-angle distribution of lost ions by means of the Doppler shape analysis as proposed in reference [16].

The optimisation of shielding, collimators and location is a critical task for GRAM. In the existing machines due to lack of space and acceptable FoV it could require a complex redesign of the current construction. In upcoming fusion burning plasmas GRAM implementation would be easier if the lost α-particle monitoring is planned in the first place. For example, in DEMO reactor this diagnostic could be imbedded in the reactor structure during the design stage, thus the α-particle loss fraction could be used as a parameter for burning control.

Acknowledgements

This work has been carried out within the framework of the EUROfusion Consortium and has received funding from the Euratom research and training programme 2014-2018 under grant agreement No 633053 and from the RCUK Energy Programme [grant No EP/P012450/1]. To obtain further information on the data and models underlying this paper please contact PublicationsManager@ukaea.uk . The views and opinions expressed herein do not necessarily reflect those of the European Commission.

References

[1] Costley A.E. 2010 IEEE Trans. Plasma Sci. **38** 2934–43

[2] Donne A.J.H., Costley A.E. and Morris A.W. Nucl. Fusion **52** (2012) 074015

[3] Darrow D. S. et al. Rev. Sci. Instrum. **75** (2004) 3566.

[4] Zweben S. J. Rev. Sci. Instrum. **57** (1986) 1774

[5] Baumel S. et al Rev. Sci. Instrum. **75** (2004) 3563.

[6] Garcia-Munoz M. et al Rev. Sci. Instrum. **80** (2009) 053003

[7] Veshchev E. A. et al Fusion Science and Technology **61** (2012) 172-184

[8] Zweben S. J. et al Nucl. Fusion **40** (2000) 91

[9] Yavorskij V. et al Physics of Plasmas **6** (1999) 3853

[10] Gassner T. et al Phys. Plasmas **19** (2012) 032115

[11] Kiptily V.G. et al Nucl. Fusion **58** (2018) 014003

[12] Goloborod'ko V. et al Nucl. Fusion **35** (1995)1523

[13] Schoepf K. et al Kerntechnik **67** (2002) 285
[14] Yavorskij V. et al J Fusion Energy **34** (2015) 774–784
[15] Polevoi et al J. Plasma Fusion Res. Ser. **5** (2002) 82
[16] Kiptily V. G. et al Fusion Technology **22** (1992) 454-460
[17] Kiptily V.G. et al Gamma Ray Spectrometry in ITER: Conceptual Design. In: Stott P.E., Gorini G., Prandoni P., Sindoni E. (eds) Diagnostics for Experimental Thermonuclear Fusion Reactors 2. Springer, Boston, MA (1998) 511-519
[18] NEA Data Bank, JENDL/AN-2005
[19] Kiptily V.G. et al Bull. Russ. Acad. Sci.: Phys. **63** (1999) 898-909
[20] Van Der Zwan L. and Geiger K.W. Nucl. Phys. **A216** (173) 188-198
[21] Kiptily V.G. et al Technical Physics **43** (1998) 471
[22] Chugunov I.N. et al Instrum. and Exp. Techniques **51** (2008) 166–170.
[23] Zoita V et al Fusion Engineering and Design **84** (2009) 2052–2057
[24] Shevelev A.E. et al Nucl. Instrum. and Meth. Phys. Res. **A830** (2016)
[25] Shevelev A.E. et al Nucl. Fusion **58** (2018) 016034
[26] Zychor I. et al Phys. Scr. **91** (2016) 064003
[27] Rigamonti D. et al Rev. Sci. Instrum. **87** (2016) 11E717
[28] Nocente et al Rev. Sci. Instrum. **87** (2016) 11E714
[29] MCNP code https://mcnp.lanl.gov/
[30] Yavoskij V et al Nucl. Fusion **43** (2003) 1077
[31] De Vries P C et al Nucl. Fusion **48** (2008) 035007
[32] Soare S et al "Conceptual design of a gamma-ray monitor for lost alpha particles in JET", 29th Symposium on Fusion Technology, Prague, September 2016.
[33] Soare S et al "Lost alpha particle monitor for JET. A conceptual design", 17th International Conference on Plasma Physics and Applications, Magurele-Bucharest, June 2017 (to be published)
[34] Moro F. et al Fusion Engineering and Design **84** (2009) 1351–1356
[35] A. J. H. Donné et al Nucl. Fusion vol. **47** (2007) 337–384, also “ITER Project Requirements” (27ZRW8 v5.3)
[36] Litaudon X. et al Nucl. Fusion 57 (2017) 102001

Figures

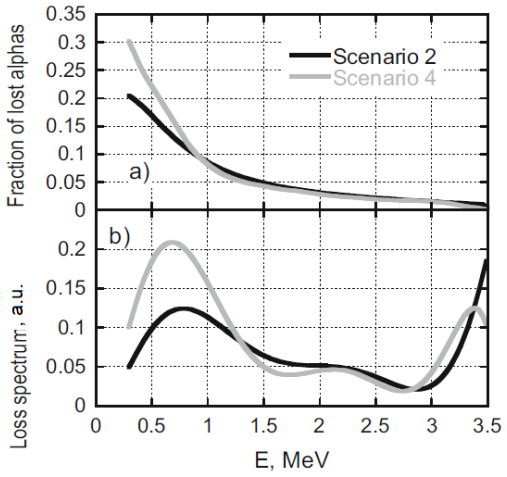


Figure 1. (a) - modelled alpha-particle loss fraction (a fraction of particles lost with energies above E) and (b) - their energy spectra for the 2nd and 4th ITER scenarios in the case of the mono-energetic source.

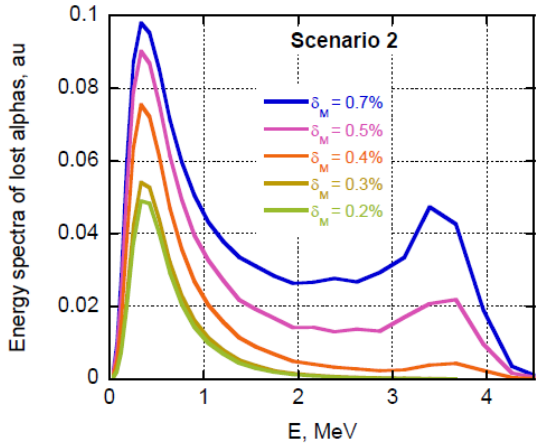


Figure 2. Energy spectra of lost alphas in 2nd scenario calculated with a real source spectrum at different TF ripple parameter δ.

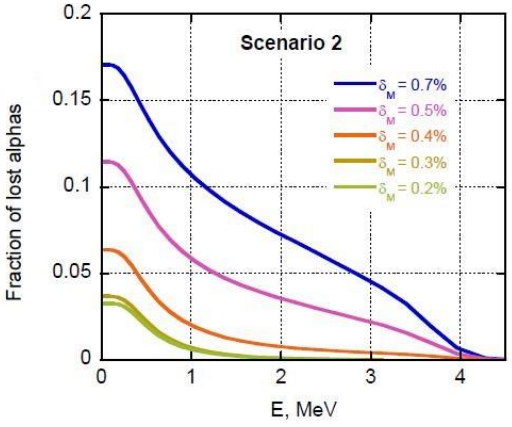


Figure 3. Fraction of fusion alphas lost via radial ripple induced diffusion in 2nd scenario calculated with a real source spectrum at different TF ripple parameter δ.

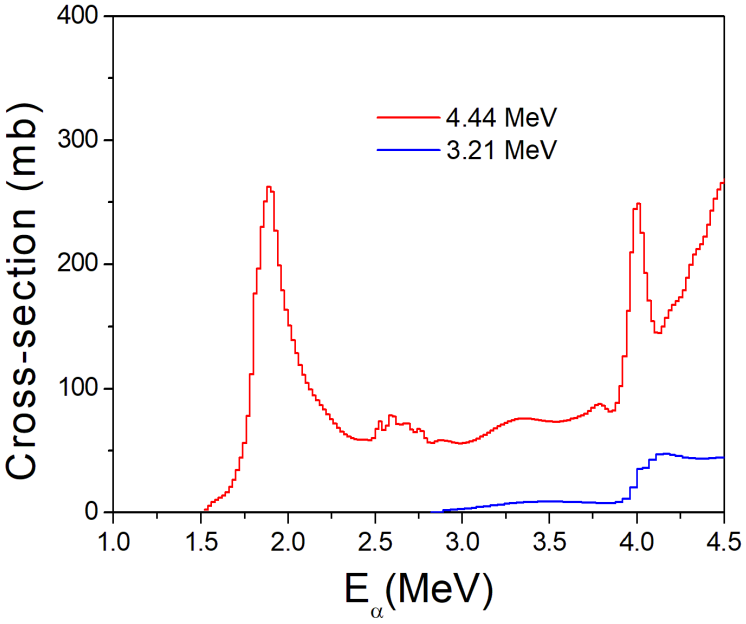


Figure 4. Partial cross-sections of the ^{9}Be(α,nγ)^{12}C reaction with population of the 1st (red line) and 2nd (blue) excited states of ^{12}C nucleus [18].

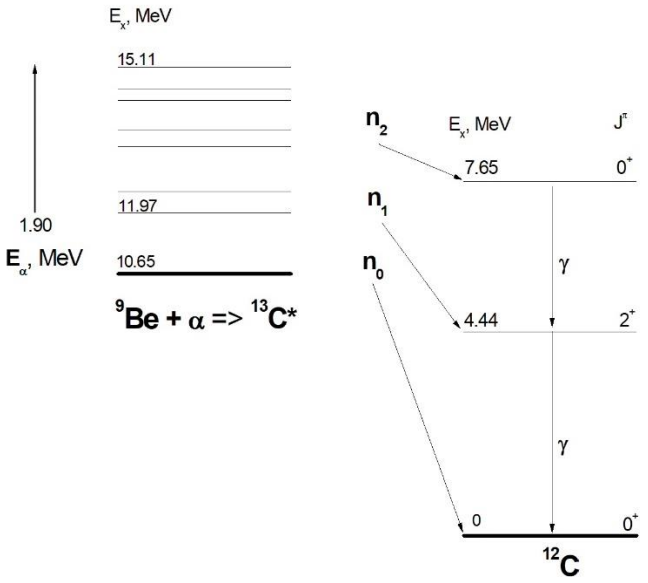


Figure 5. Scheme of the excitation of ^{12}C nucleus due to the ^{9}Be(α,nγ)^{12}C reaction.

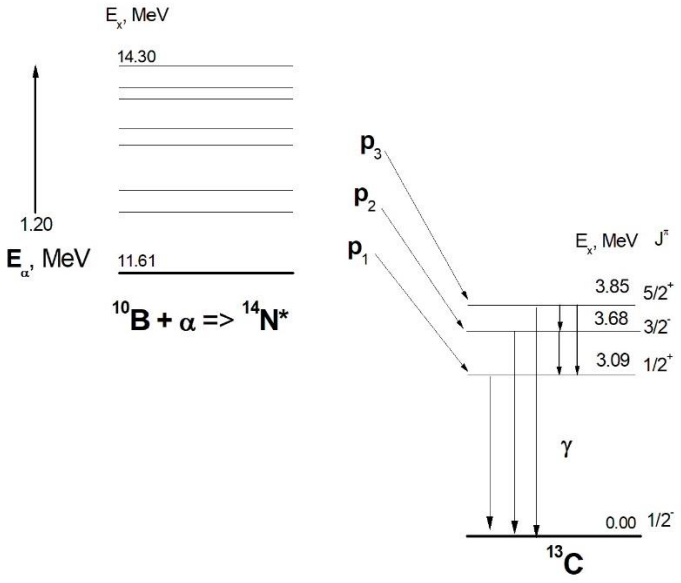


Figure 6. Scheme of the excitation of ^{13}C nucleus due to the ^{10}B(α,pγ)^{13}C reaction.

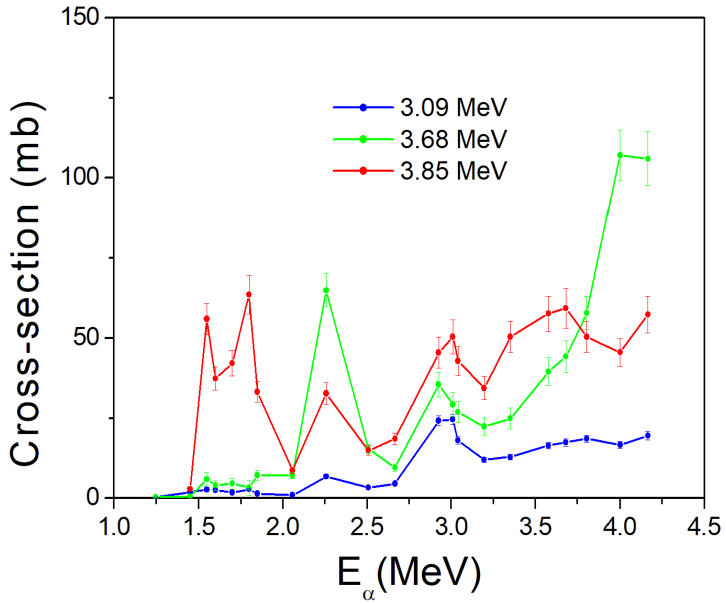


Figure 7. Partial cross-sections of the ^{10}B(α,pγ)^{13}C reaction with population of the first three levels of ^{13}C nucleus [19].

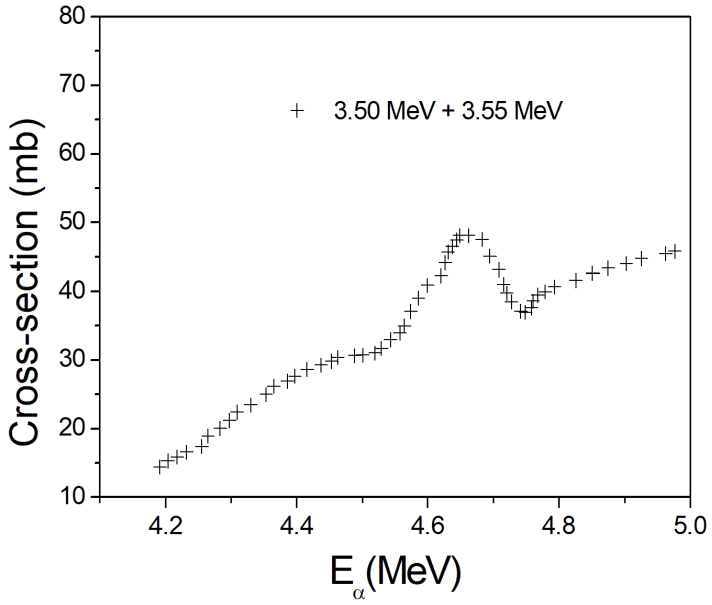


Figure 8. Integral cross-section of the $^{10}B(\alpha,n\gamma)^{13}N$ reaction with population of the 2nd and 3rd excited states of ^{13}N nucleus [20].

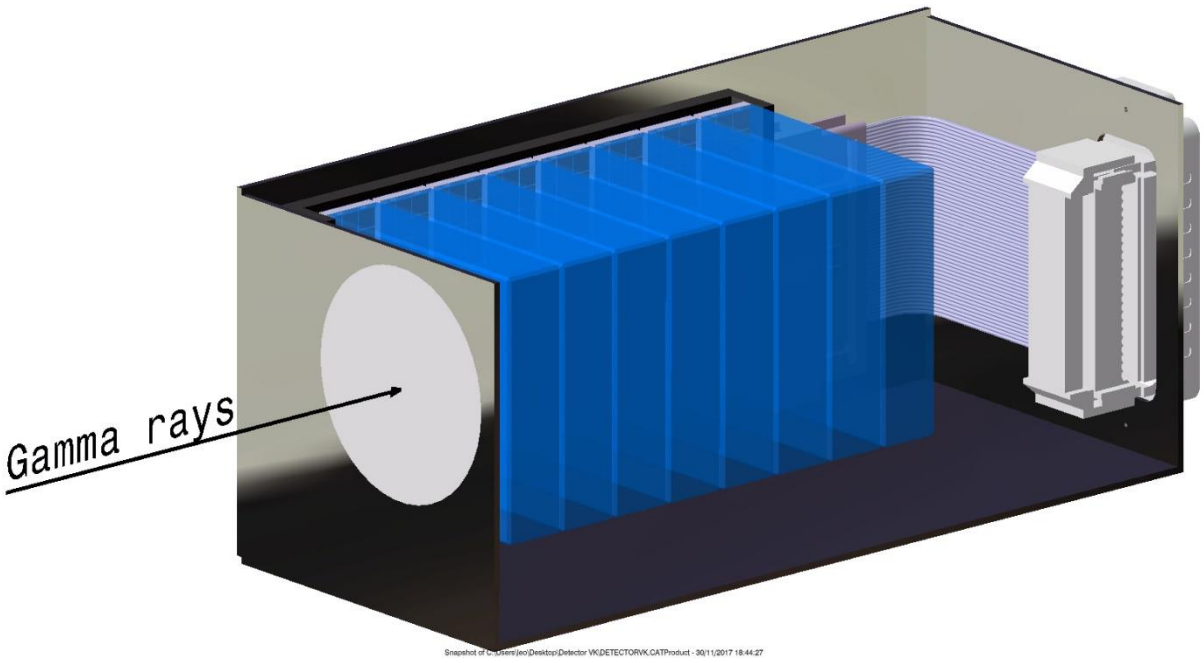


Figure 9. Schematic representation of the γ-ray spectrometer GRITER, which consist of 8 optically isolated scintillators connected with Si photo-multipliers and readout module.

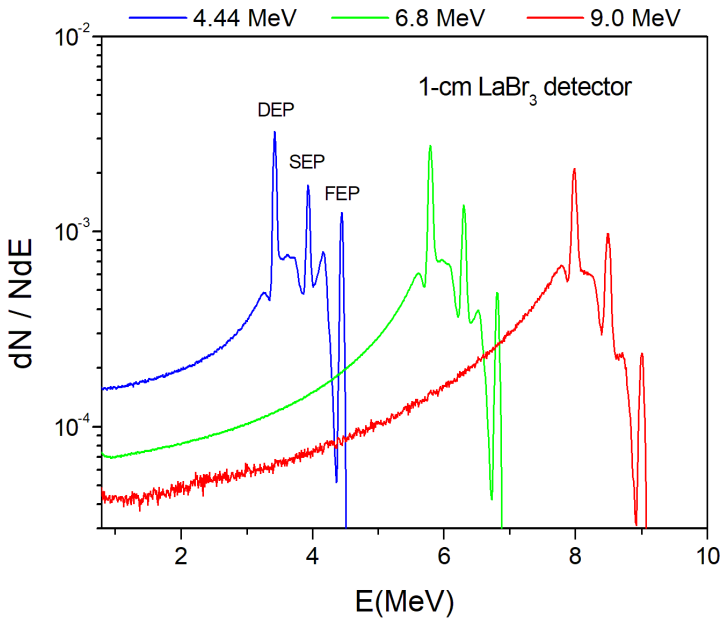


Figure 10. Calculated response functions (au) of $LaBr_3$ γ-ray detector with dimensions 1cm x 4cm x 4 cm; FEP – full energy peak; SEP – single escape energy peak at $E_\gamma - m_e c^2$; DEP – double escape energy peak at $E_\gamma - 2m_e c^2$

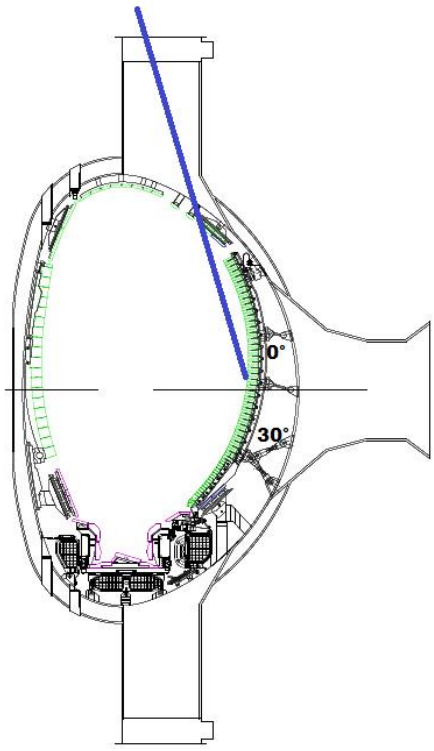


Figure 11. A generic LoS proposed for GRAM in JET

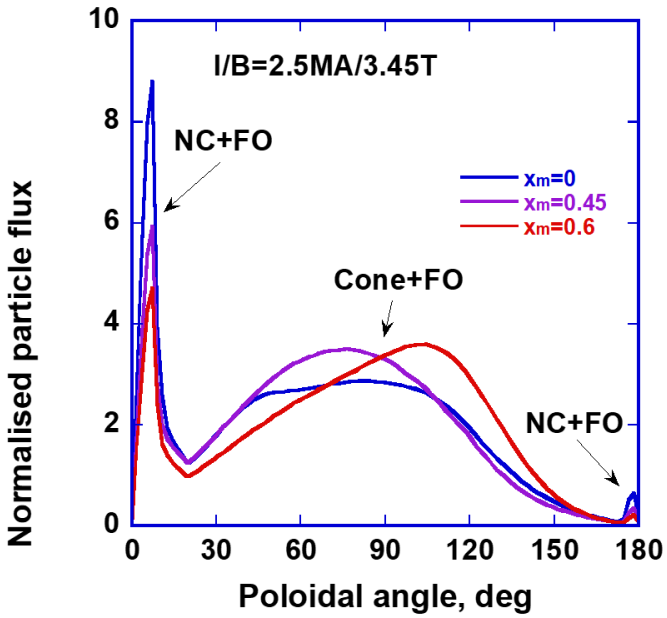


Figure 12. Normalised flux of total α-particle losses (FO, neoclassical and cone) in JET discharge calculated at different current hole size [30].

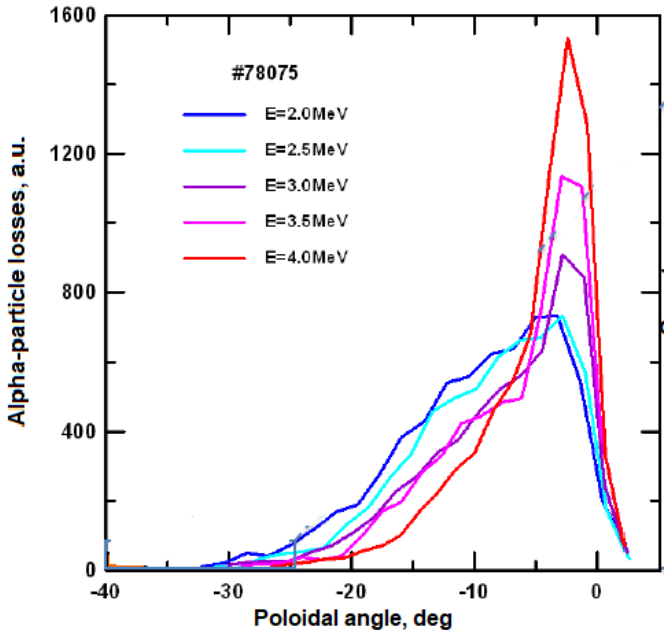


Figure 13. Result of the α-particle classical losses modelling in JET DT discharge, which is equivalent to the deuterium discharge #78075: the loss rate vs poloidal angle for alphas in the energy range 2 – 4 MeV.

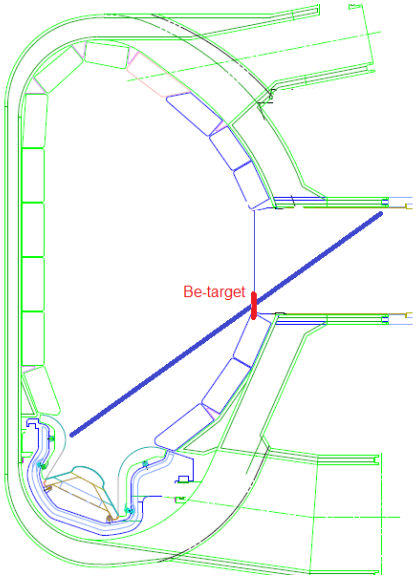


Figure 14. A generic LoS proposed for GRAM in ITER; the diagnostic could occupy the port with RNC in-port detectors.

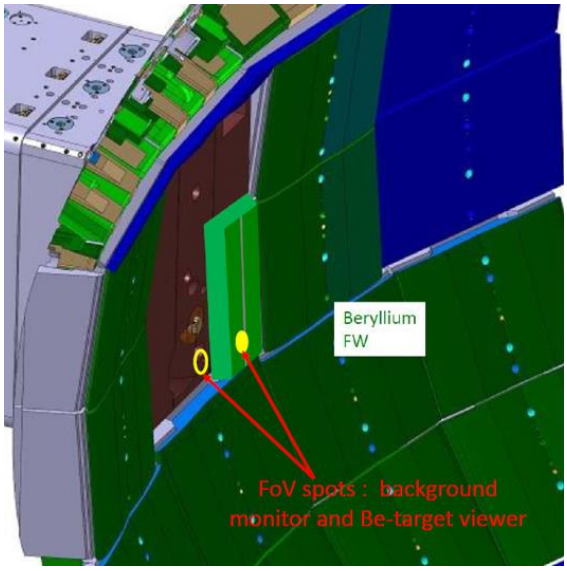


Figure 15. A generic target for GRAM in ITER – a typical Be-tile could be installed in the ITER port; yellow spot – a view of target by the α-particle monitor; yellow circle – an area seen by background monitor.

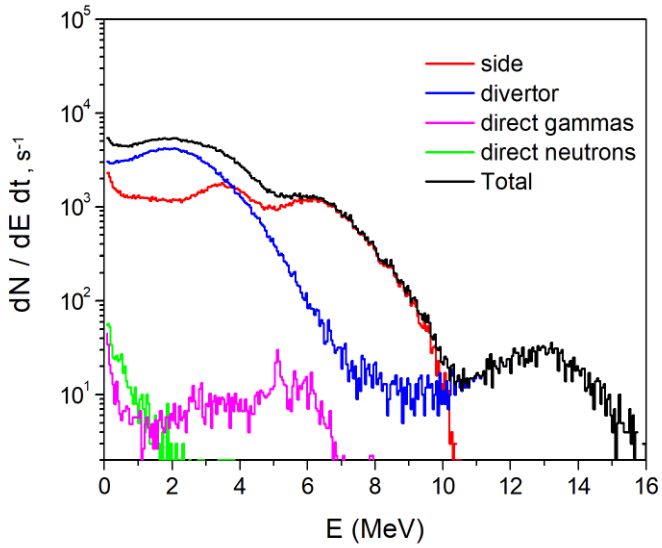


Figure 16. Background spectra calculated for the front GRITER detector section (dE=50 keV); components related to γ-rays, which irradiate the detector directly, from side and coming from W-divertor are shown.

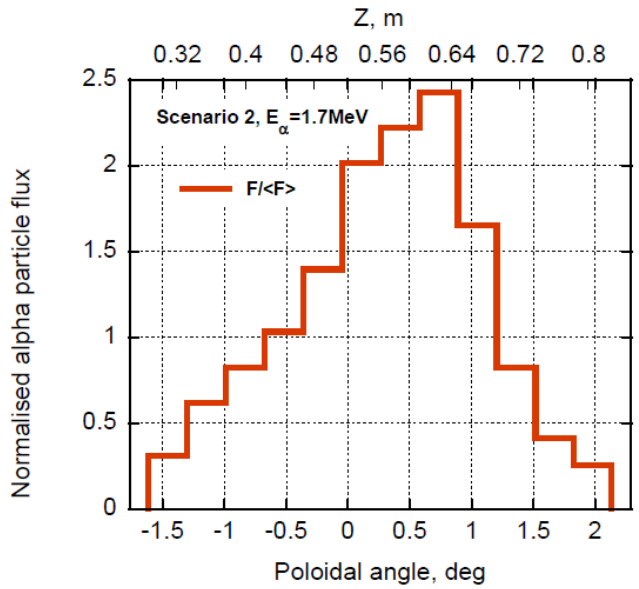


Figure 17. Alpha-particle losses in ITER related to scenario #2; normalised loss flux vs poloidal angle for alphas with $E_\alpha > 1.7$ MeV; vertical coordinate $Z \approx 0.25 + 5.25 \sin\theta$ (m).

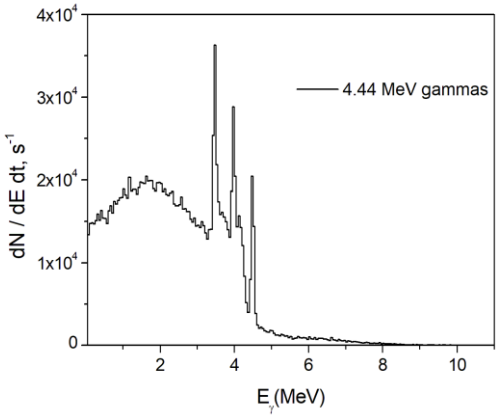


Figure 18. Energy spectra calculated for GRAM with 125-cm PW neutron attenuator (dE=50 keV); GRITER is in the anti-coincidence mode; energy resolution $\Delta E_\gamma/E_\gamma \approx 4\%$

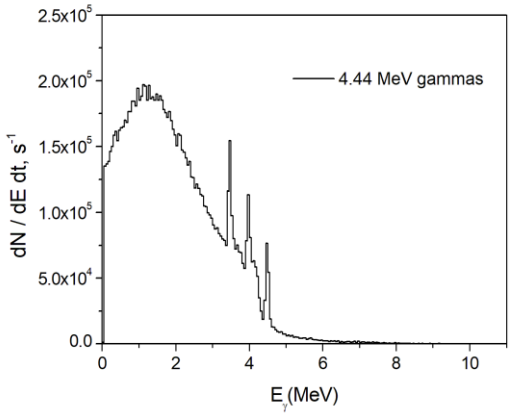


Figure 19. Energy spectra calculated for GRAM with 125-cm LiH neutron attenuator (dE=50 keV); GRITER is in the anti-coincidence mode; energy resolution $\Delta E_\gamma/E_\gamma \approx 4\%$